

Deep Space Network

214 Pseudo-Noise and Regenerative Ranging

Document Owner:

Approved by:

Signature Provided 10/27/2015

Signature Provided 06/02/2015

Andrew O’Dea
Telemetry, Tracking, and Command
System Engineer

Date

Timothy Pham
Communications Systems Chief
Engineer

Date

Prepared By:

Released by:

Signature Provided 06/02/2015

Signature Provided 10/27/2015

Peter Kinman
Telecommunications Technical
Consultant

Date

Christine Chang
DSN Document Release Authority

Date

DSN No. **810-005, 214, Rev. A**
Issue Date: October 28, 2015
JPL D-19379; CL#15-4729

Jet Propulsion Laboratory
California Institute of Technology

*Users must ensure that they are using the current version in DSN Telecommunications Link Design Handbook website:
<http://deepspace.jpl.nasa.gov/dsndocs/810-005/>*

© <2015> California Institute of Technology.
U.S. Government sponsorship acknowledged.

Review Acknowledgment

By signing below, the signatories acknowledge that they have reviewed this document and provided comments, if any, to the signatories on the Cover Page.

Signature Provided

06/02/2015

Signature Not Provided

Jeff Berner
DSN Project Chief Engineer

Date

Scott Bryant
DSN Ranging Cognizant Development
Engineer

Date

Contents

<u>Section</u>	<u>Page</u>
1. Introduction.....	6
1.1 Purpose.....	6
1.2 Scope.....	6
2. General Information.....	6
2.1 System Description.....	7
2.2 Parameters Specified for Ranging Operations.....	8
2.2.1 Range Clock.....	9
2.2.2 Ranging Signal Structure.....	9
2.2.3 Integration Time.....	13
2.2.4 Uplink Ranging Modulation Index.....	13
2.2.5 Tolerance.....	13
2.3 Allocation of Link Power.....	13
2.3.1 Uplink.....	13
2.3.2 Downlink.....	14
2.4 Uplink Spectrum.....	18
2.5 Range Measurement Performance.....	20
2.5.1 Cross-Correlation Factors.....	21
2.5.2 Range Measurement Error Due to Thermal Noise.....	22
2.5.3 Probability of Acquisition.....	25
2.5.4 Processing a Set of Range Measurements.....	29
2.5.5 Comparison of PN Ranging and Sequential Ranging.....	30
2.5.6 Non-Coherent Operation.....	31
2.6 Range Corrections.....	32
2.6.1 DSS Delay.....	33
2.6.2 Z-Correction.....	33
2.7 Total Error for Range Measurement.....	34
References.....	35

Illustrations

<u>Figure</u>	<u>Page</u>
Figure 1. The DSN Ranging System Architecture.....	7
Figure 2. PN Ranging Signal for the JPL PN Code.....	12
Figure 3. Uplink Spectrum for the JPL PN Code Ranging Signal.....	19
Figure 4. Uplink Ranging Filter Frequency Response.....	20
Figure 5. Standard Deviation of Range Measurement Error for the JPL and T4B Codes.....	24
Figure 6. Standard Deviation of Range Measurement Error for the T2B Code	25
Figure 7. Probability of Acquisition for the JPL PN Code and the T4B Code.....	28
Figure 8. Probability of Acquisition for the T2B Code	29
Figure 9. Comparison of Sequential Ranging and PN Ranging	31
Figure 10. DSS Delay Calibration, Uplink and Downlink in a Common Band	34
Figure 11. DSS Delay Calibration, Uplink and Downlink in Different Bands.....	34

Tables

<u>Table</u>	<u>Page</u>
Table 1. Component Codes.....	10
Table 2. Definition of $\alpha(\cdot)$ and $\beta(\cdot)$	14
Table 3. Cross-Correlation Factors, JPL PN Code	21
Table 4. Cross-Correlation Factors, T4B (Reference 5)	21
Table 5. Cross-Correlation Factors, T2B (Reference 5)	22
Table 6. Required $(A_c R_n)^2 \cdot T \cdot P_R / N_0$ (in decibels) for Given λ_n and P_n	27
Table 7. Parameters for Equation (45).....	27

1. Introduction

1.1 Purpose

This module describes capabilities of the Deep Space Network (DSN) for pseudo-noise (PN) ranging. These capabilities are available within the 70-m, the 34-m High Efficiency (HEF), and the 34-m Beam Waveguide (BWG) subnets. Performance depends on whether the spacecraft transponder uses a turn-around (non-regenerative) ranging channel or a regenerative ranging channel. Performance parameters are provided for both cases.

1.2 Scope

The material contained in this module covers the PN ranging system that may be utilized by both near-Earth and deep-space missions. This document describes those parameters and operational considerations that are independent of the particular antenna being used to provide the telecommunications link. For antenna-dependent parameters, refer to module 101, 103, or 104 of this handbook. The other ranging scheme employed by the DSN is sequential ranging, described in module 203.

An overview of the ranging system is given in Section 2.1. The parameters to be specified for ranging operations are explained in Section 2.2. The distribution of link power is characterized in Section 2.3. The spectrum of an uplink carrier modulated by a PN ranging signal is discussed in Section 2.4. The performance of turn-around and regenerative ranging is summarized in Section 2.5. The case of non-coherent ranging is also discussed there. Section 2.6 describes the corrections required to determine the actual range to a spacecraft. Error contributions of the ground instrumentation are discussed in Section 2.7.

2. General Information

The DSN ranging system provides a ranging signal for measuring the round-trip light time (RTLTL) between a Deep Space Station (DSS) and a spacecraft. The ranging signal of interest in this module is a logical combination of a range clock and several PN codes. The DSS transmits an uplink carrier that has been phase modulated by this ranging signal. The modulated uplink carrier is received and processed by the spacecraft transponder. The ranging channel of the transponder may be either a relatively simple turn-around (non-regenerative) channel or a regenerative channel. In either case, the downlink carrier is phase modulated by a copy of the uplink ranging signal. (Regenerative ranging has a performance advantage over turn-around ranging because with regeneration there is less noise accompanying the ranging signal onto the downlink.) Back at the DSS, the downlink carrier is demodulated. The received ranging signal is correlated with a local model of the range clock. There is a measurement ambiguity associated with this correlation, since the range clock is a periodic signal. This ambiguity is resolved by also correlating the received ranging signal with a local model of each of the individual PN codes that is a component of the ranging signal. In coherent operation, these local models will match the frequencies of their counterparts in the received ranging signal by virtue of Doppler rate-aiding.

2.1 System Description

The DSN ranging system records the phase of the ranging signal that is transmitted and measures the phase of the ranging signal that returns. Both recorded phase values (that of the uplink ranging signal and that of the downlink ranging signal) apply to a common instant in time, an epoch of the 1-pulse per second timing reference, which becomes the common time tag. From these two phases plus knowledge of the history of the transmitted range-clock frequency, a user may compute the two-way time delay (Reference 1). This two-way time delay applies to a signal arriving at the DSS at the instant specified by the time tag.

The architecture for the DSN ranging system is shown in Figure 1. The ranging signal originates in the Uplink Subsystem (UPL). The returned signal is processed in the Downlink Tracking and Telemetry Subsystem (DTT). Both the UPL and the DTT are located at the Deep Space Communications Complex (DSCC).

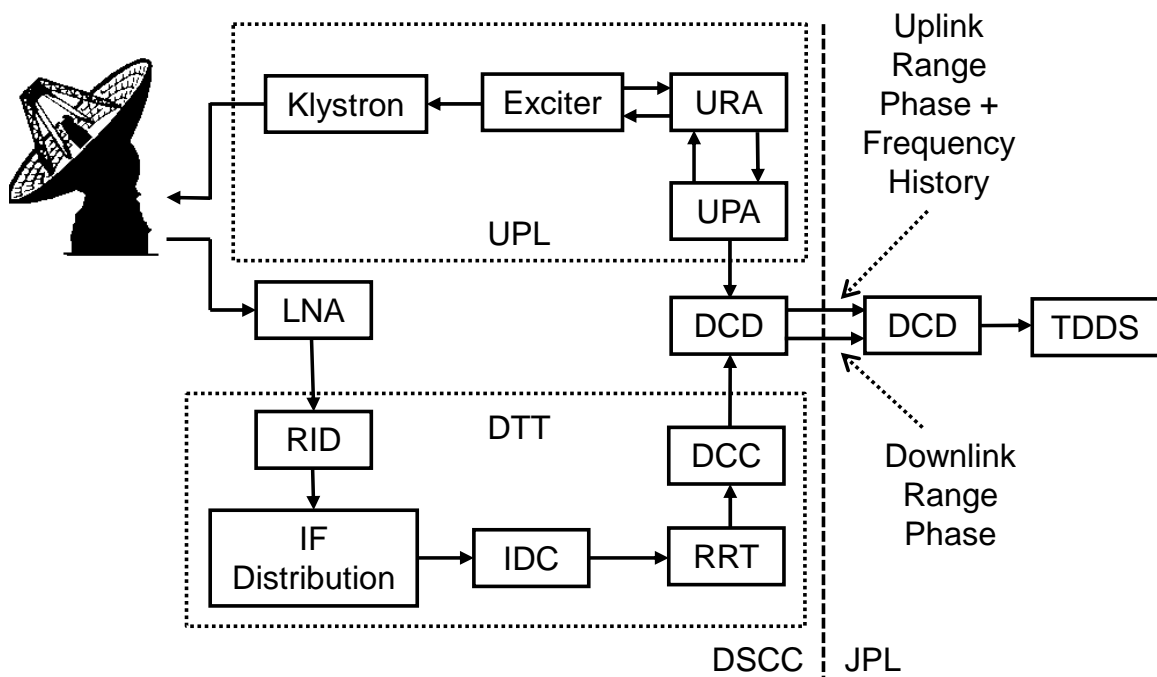


Figure 1. The DSN Ranging System Architecture

The signal processing in the UPL may be summarized as follows. The Uplink Ranging Assembly (URA) receives from the exciter a reference clock that is coherently related to the uplink carrier. The URA synthesizes the range clock from the reference clock, and this range clock is thus coherently related to the uplink carrier. The URA generates the ranging signal, which is the range clock modified by additional signal structure that makes possible resolution of the phase ambiguity. The URA passes this ranging signal to the exciter. A sample of the uplink phase, which is required for the delay measurement, is passed from the URA to the Uplink Processor Assembly (UPA). The exciter modulates the uplink carrier with the ranging signal. The klystron supplies the final stage of power amplification for the uplink carrier.

The downlink carrier, after amplification within the Low-Noise Amplifier (LNA), passes to the DTT. Frequency down-conversion to an intermediate frequency (IF) takes place in the RF-to-IF Downconverter (RID). The IF signal is sent to an IF-to-Digital Converter (IDC). Demodulation of the IF carrier occurs in the Receiver, Ranging and Telemetry (RRT) processor. Also within the RRT, the correlation of the received, baseband ranging signal with a local model produces a measurement of the downlink phase. This downlink phase is passed to the Downlink Channel Controller (DCC).

Uplink phase samples, each corresponding to an epoch of the 1-PPS (pulse per second) clock, are passed from the UPA, via the Data Capture and Delivery (DCD) software, to the Tracking Data Delivery Subsystem (TDDS), located in Pasadena. The DCC passes the downlink phase measurement and its time tag (an epoch of the 1-PPS clock), via the DCD, to the TDDS. A history of the uplink range clock's frequency is also needed for the calculation of the two-way time delay. Since the uplink range clock is coherently related to the uplink carrier, this necessary information can be derived from the history of the uplink carrier frequency, which is supplied by the UPA to the TDDS. All data required for the two-way delay calculation are archived by the TDDS for later use by a navigation team or other users.

The IDC, RRT, and DCC required for the processing of a downlink carrier are located within a Downlink Channel Processing Cabinet (DCPC). Each DCPC supports a single channel. For spacecraft with multiple channels (for example, X-band and Ka-band), or for multiple spacecraft within a single antenna beamwidth, multiple DCPCs will be assigned to that antenna.

The phase values are delivered to users in units of phase called the Range Unit (RU). Range units are defined, for historical reasons related to hardware design, as two cycles of the S-band uplink frequency (the only frequency band that was in use when the definition was established). Since 2 cycles of a 2-GHz (S-band) frequency occupy one nanosecond, one RU of phase delay corresponds approximately to 1 ns of time delay, and this is true whether the uplink carrier is in the S band or the X band. A user may convert a two-way phase delay in RU into a two-way time delay as follows:

$$\text{Two-way Time Delay} = \begin{cases} \frac{2 \times RU}{f_S}, & \text{S-band uplink} \\ \frac{749}{221} \cdot \frac{2 \times RU}{f_X}, & \text{X-band uplink} \end{cases} \quad (1)$$

where RU is the two-way phase delay in range units, f_S is the frequency of an S-band uplink carrier, and f_X is the frequency of an X-band uplink carrier. For example, if the uplink carrier is in the X band with a frequency of 7.160 GHz and the two-way phase delay has been calculated as 6,500,000 RU, then the two-way time delay is 6,153,467 ns.

2.2 *Parameters Specified for Ranging Operations*

The following subsections present the parameters that are required in ranging operations.

2.2.1 Range Clock

The range clock is a periodic signal, usually a sinewave. It represents the most visible component of the ranging signal for PN ranging operation. The range clock on the uplink is coherently related to the uplink carrier. The frequency f_{RC} of this range clock is related to that of the uplink carrier by

$$f_{RC} = \begin{cases} \frac{1}{128 \cdot 2^k} \times f_S, & \text{S-band uplink} \\ \frac{221}{749} \times \frac{1}{128 \cdot 2^k} \times f_X, & \text{X-band uplink} \end{cases} \quad (2)$$

where f_S is the frequency of an S-band uplink carrier and f_X is the frequency of an X-band uplink carrier. The component number k (an integer) is limited to $k \leq 10$. The most commonly used range-clock frequency is near 1 MHz, corresponding to $k = 4$. The exact value of f_{RC} depends on the channel assignment and on whether there is Doppler compensation on the uplink. A k of 5 results in a range-clock frequency of about 500 kHz, a k of 6 results in a range-clock frequency of about 250 kHz, etc.

In the interest of uplink spectrum conservation, all range clocks corresponding to $k \leq 6$ will be sinewaves. However, range clocks corresponding to $7 \leq k \leq 10$ may be squarewaves. The range measurement error due to thermal noise is smaller for higher range-clock frequencies (i.e., lower component numbers), so it is expected that most missions will use sinewave range clocks.

2.2.2 Ranging Signal Structure

The PN ranging signal is based on a composite code. The composite code, in turn, is built out of component codes. These codes are generated in software (Reference 2), and there is a great deal of flexibility in the design of these codes. Below the commonly used set of component codes is described. Then for each of three different ranging signals, a formula is given for constructing the composite code out of the component codes.

2.2.2.1 Component Codes

Table 1 lists the component codes that are commonly used in ranging. In this table, a component code is represented as a finite-length sequence of bits. The length of the n -th component code is denoted λ_n for $1 \leq n \leq 6$. The lengths are: $\lambda_1 = 2$, $\lambda_2 = 7$, $\lambda_3 = 11$, $\lambda_4 = 15$, $\lambda_5 = 19$, and $\lambda_6 = 23$. (The first component code is the 2-bit sequence representing the range clock.) The n -th component code is denoted $b_n(i)$, where i represents a discrete-time index, $0 \leq i < \lambda_n$. The proper order of each of these component codes is determined by reading the bits in each row from left to right. So, for example, the first three bits of $b_3(\cdot)$ are all 1s and the final bit is a 0.

It is also useful to represent each component code as a sequence of chips (with the bipolar values ± 1).

$$c_n(i) = 2 b_n(i) - 1 \quad (3)$$

where $c_n(i) = \pm 1$. Equation (3) translates a binary 1 into +1 and a logical 0 into -1.

Table 1. Component Codes

b_1	1, 0
b_2	1, 1, 1, 0, 0, 1, 0
b_3	1, 1, 1, 0, 0, 0, 1, 0, 1, 1, 0
b_4	1, 1, 1, 1, 0, 0, 0, 1, 0, 0, 1, 1, 0, 1, 0
b_5	1, 1, 1, 1, 0, 1, 0, 1, 0, 0, 0, 0, 1, 1, 0, 1, 1, 0, 0
b_6	1, 1, 1, 1, 1, 0, 1, 0, 1, 1, 0, 0, 1, 1, 0, 0, 1, 0, 1, 0, 0, 0, 0

2.2.2.2 JPL PN Code

The so-called “JPL PN code” is the first composite code to be implemented and validated with the current ranging instrumentation in the DSN. This range code currently enjoys the status of the default code for PN ranging. Following is an explanation of how this composite code is generated from the component codes listed in Table 1.

For each finite-length PN code $b_n(i)$, a periodic code $b_n'(i)$ of period λ_n is formed by endless repetition:

$$b_n'(i) = b_n(i \bmod \lambda_n) \quad (4)$$

where $b_n'(i)$ is binary valued. In this document, the prime (') indicates a periodic sequence (made from a finite-length sequence by periodic extension).

The composite code is

$$b'(i) = b_1'(i) \cup [b_2'(i) \cap b_3'(i) \cap b_4'(i) \cap b_5'(i) \cap b_6'(i)] \quad (5)$$

where \cup and \cap are the logical OR and logical AND operators, respectively. Since the component code lengths λ_n ($1 \leq n \leq 6$) are relatively prime, the period L (in bits) of the composite code is the product of the component code lengths. That is,

$$b'(i + L) = b'(i) \quad (6)$$

where

$$L = \prod_{n=1}^6 \lambda_n = 1,009,470 \quad (7)$$

The periodic chip sequence corresponding to the periodic bit sequence $b'(i)$ is

$$c'(i) = 2 b'(i) - 1 \quad (8)$$

where $b'(i)$ is the periodic bit sequence of Equation (5). $c'(i)$ is bipolar, $c'(i) = \pm 1$.

In this design a large L is obtained from relatively small component code lengths. A large L is necessary for resolution of the range ambiguity, yet small λ_n are needed for a

practical implementation of the correlators at the receiver. The ambiguity resolution of this code is given by

$$\text{ambiguity resolution} = \frac{c \cdot L}{4f_{RC}} \quad (9)$$

For a range clock of approximately 1 MHz ($k = 4$), the ambiguity resolution is 75,660 km.

An important property of this composite code is that it approximates a sequence of period 2 bits. The composite code equals $b_1'(i)$, the first component with a period of 2 bits, most of the time. The effect of the other 5 component codes is to invert a small fraction (1/32) of the logical 0s in $b_1'(i)$. Since $b_1'(i)$ corresponds to the range clock, the composite code may be viewed as the range clock with an occasional inversion of a logical 0.

Most of this ranging signal's power lies at the range-clock frequency. This is desirable, since the accuracy of the range measurement is set by a correlation against a local model of the range clock. The occasional inversion is necessary to resolve the range ambiguity, but for this purpose the inversions need not be frequent.

2.2.2.3 *CCSDS T4B Code*

The Consultative Committee for Space Data Systems (CCSDS) recommends a composite code called T4B for use in deep-space ranging (Reference 3). The T4B code employs the same set of component codes that are used by the JPL PN code (Table 1). The T4B code is constructed from the component chip sequences:

$$c_n'(i) = c_n(i \bmod \lambda_n) \quad (10)$$

where $c_n(\cdot) = \pm 1$ is the chip sequence of length λ_n for the n -th component code, as given by Equation (3), and $c_n'(\cdot)$ is its periodic extension. The periodic, composite chip sequence $c'(i)$ is computed from the components $c_n'(i)$ as follows:

$$c'(i) = \text{sign}[4c_1'(i) + c_2'(i) - c_3'(i) - c_4'(i) + c_5'(i) - c_6'(i)] \quad (11)$$

where $c'(i) = \pm 1$ and where $\text{sign}[\cdot]$ is the algebraic sign of its argument. The period of the composite code $c'(i)$ equals L , as given in Equation (7). The ambiguity resolution of this code is the same as that for the JPL PN code; this resolution is given in Equation (9).

As suggested by Equation (11), the range clock $c_1'(i)$ has a disproportionate influence on the composite code $c'(i)$. The composite code may be viewed as the range clock with an occasional inversion of a chip. (With the T4B code, unlike the JPL PN code, the inversion may go in either direction: $-1 \rightarrow +1$ or $+1 \rightarrow -1$.) As with the JPL PN code, most of the ranging signal's power lies at the range-clock frequency. As indicated in Section 2.5, the performance of the T4B code is close to that of the JPL PN code.

2.2.2.4 *CCSDS T2B Code*

The CCSDS recommends a second composite code, called T2B, which provides an alternative to the T4B code in performance trade-off space (Reference 3). The T2B code employs the same set of component codes (Table 1) that are used by the JPL PN code and the T4B code. The periodic, composite chip sequence $c'(i)$ for the T2B code is computed from the components $c_n'(i)$ as follows:

$$c'(i) = \text{sign}[2c_1'(i) + c_2'(i) - c_3'(i) - c_4'(i) + c_5'(i) - c_6'(i)] \quad (12)$$

The period of the T2B code equals L , as given in Equation (7). The ambiguity resolution of this code is the same as that for the T4B code and the JPL PN code; this resolution is given in Equation (9).

In the construction of the T2B code, using Equation (12), the range clock $c_1'(i)$ gets only 2 “votes”, whereas in the construction of the T4B code, using Equation (11), the range clock gets 4 “votes”. As a result, the T2B code places less power in the range clock. The T2B code will therefore generally produce a less accurate range measurement than the T4B code; however, the T2B code will achieve a better probability of acquisition for smaller received power levels.

2.2.2.5 Conversion of Composite Code to a Ranging Signal

The PN ranging signal is created from the composite code by translating each $+1$ chip of the composite code into a positive half-cycle of a sinewave and each -1 into a negative half-cycle of a sinewave. (However, when the range-clock frequency is 125 kHz or less, the half-cycles may be from a squarewave, rather than a sinewave.)

For example, the ranging signal created from the JPL PN code would look as shown in Figure 2. The parameter T_c represents the chip period, so only the first 8 chips are represented in Figure 2. The range-clock frequency equals $1/(2T_c)$.

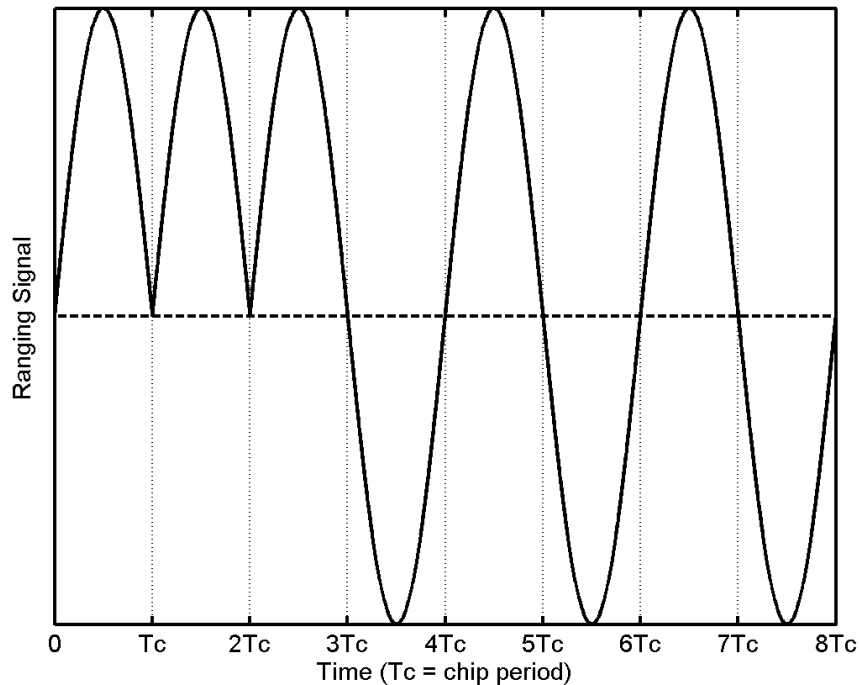


Figure 2. PN Ranging Signal for the JPL PN Code

2.2.3 *Integration Time*

The integration time T should be large enough that the probability of range measurement acquisition is close to 1.0 and the range error due to downlink thermal noise is small (see Section 2.5). In the special case of non-coherent ranging, the presence of a frequency mismatch between the received ranging signal and the local model means that there is also reason to keep T relatively small, so that an optimum T should be carefully chosen for non-coherent ranging.

2.2.4 *Uplink Ranging Modulation Index*

The uplink ranging modulation index is chosen to get a suitable distribution of power among the ranging and command sidebands and the residual carrier on the uplink (see Section 2.3). With turn-around (non-regenerative) ranging, the uplink ranging modulation index also affects the distribution of power on the downlink carrier.

2.2.5 *Tolerance*

The tolerance plays a role in deciding whether to judge range acquisitions as valid or invalid. For any given range acquisition, the ratio P_R/N_0 of the downlink ranging signal power to the noise spectral density is measured. From this measured P_R/N_0 , an estimate of the probability of acquisition P_{acq} is calculated. Section 2.5 describes the calculation of the P_{acq} from P_R/N_0 .

Tolerance may be selected over the range of 0.0% to 100.0%. As an example, if the tolerance is set to 0.0%, all range acquisitions will be declared valid. Alternately, if the tolerance is set to 100.0%, all range acquisitions will be declared invalid. The default value for tolerance is 99%. A tolerance of 99% will flag acquisitions that have a 99% or better chance of being good as valid, and the rest as invalid. An acquisition is declared valid or invalid depending upon the following criteria:

$P_{acq}(\%) \geq \text{Tolerance}$ *results in* Acquisition declared valid

$P_{acq}(\%) < \text{Tolerance}$ *results in* Acquisition declared invalid.

2.3 *Allocation of Link Power*

The equations governing the allocation of power on uplink and downlink depend on whether the range clock is sinewave or squarewave. Most often, the range clock will be sinewave; but for the sake of completeness, both cases are considered here. In order to achieve economy of expression, it is advantageous to introduce the functional definitions of Table 2. Bessel functions of the first kind of order 0 and 1 are denoted $J_0(\cdot)$ and $J_1(\cdot)$.

2.3.1 *Uplink*

The equations of this subsection represent the case where a PN ranging signal and a command signal are simultaneously present on the uplink carrier. The ranging signal may employ either a sinewave range clock (“sinewave” in Table 2) or a squarewave range clock (“bipolar” in Table 2). The command may be on a sinewave subcarrier (“sinewave” in Table 2) or may be a stream of symbols directly modulating the carrier (“bipolar” in Table 2). The carrier suppression is

$$\frac{P_C}{P_T} = \alpha^2(\phi_r) \cdot \alpha^2(\phi_c) \quad (13)$$

The ratio of available ranging signal power to total power is

$$\frac{P_R}{P_T} = \beta^2(\phi_r) \cdot \alpha^2(\phi_c) \quad (14)$$

The ratio of available command (data) signal power to total power is

$$\frac{P_D}{P_T} = \beta^2(\phi_c) \cdot \alpha^2(\phi_r) \quad (15)$$

Table 2 defines the functions $\alpha(\cdot)$ and $\beta(\cdot)$. As an example, when the range clock is a sinewave, $\alpha(\phi_r) = J_0(\sqrt{2} \phi_r)$ and $\beta(\phi_r) = \sqrt{2} J_1(\sqrt{2} \phi_r)$.

Table 2. Definition of $\alpha(\cdot)$ and $\beta(\cdot)$

Signal	$\alpha(\psi)$	$\beta(\psi)$
sinewave	$J_0(\sqrt{2} \psi)$	$\sqrt{2} J_1(\sqrt{2} \psi)$
bipolar (squarewave)	$\cos(\psi)$	$\sin(\psi)$

In these equations, ϕ_r is the uplink ranging modulation index in radians rms and ϕ_c is the command modulation index in radians rms. If command is absent, $\phi_c = 0$ and $\alpha(\phi_c) = 1$, so the factor representing command modulation in Equations (13) and (14) is simply ignored. If command is absent, Equation (15) is not applicable.

2.3.2 *Downlink*

The equations for power allocation on the downlink depend on whether the spacecraft transponder has a turn-around (non-regenerative) ranging channel or a regenerative ranging channel.

2.3.2.1 *Turn-Around (Non-Regenerative) Ranging*

A turn-around ranging channel demodulates the uplink carrier, filters the baseband signal, applies automatic gain control, and then re-modulates the baseband signal onto the downlink carrier. The automatic gain control (AGC) serves the important purpose of ensuring that the downlink carrier suppression is approximately constant, independent of received uplink signal level. A typical bandwidth for this turn-around channel is 1.5 MHz: wide enough to pass a 1-MHz range clock. Unfortunately, substantial thermal noise from the uplink also passes through this channel. In many deep space scenarios, the thermal noise dominates over the ranging signal in this turn-around channel. Moreover, command signal from the uplink may pass through this ranging channel. In general, then, noise and command signal as well as

the desired ranging signal are modulated on the downlink carrier whenever the ranging channel is active. A proper analysis must account for all significant contributors (Reference 4).

Three transponder parameters affect the performance of turn-around ranging.

These are:

B_R	Noise-equivalent bandwidth of ranging channel, Hz
θ_d or Ψ_d	Design value of the downlink ranging modulation index, rad rms (θ_d) or rad peak (Ψ_d)
θ_t	Telemetry modulation index, rad

The design value of the downlink ranging modulation index is denoted here either θ_d (rad rms) or Ψ_d (rad peak), depending on the design of the AGC in the ranging channel. In some transponders, the AGC is designed to keep constant the rms voltage at the AGC output, and then θ_d (rad rms) will be employed in calculating the allocation of the downlink power. In other transponders, the AGC is designed to keep constant the average of the absolute value of the voltage at the AGC output, and then Ψ_d (rad peak) will be employed in calculating the allocation of the downlink power. Both cases are treated below. The design value (θ_d or Ψ_d) of the downlink ranging modulation index is different, in general, from the *effective* downlink ranging signal modulation index (called θ_r), as explained below.

For both types of AGC, the carrier suppression is

$$\frac{P_C}{P_T} = \alpha^2(\theta_r) \cdot \alpha^2(\theta_c) \cdot e^{-\theta_n^2} \cdot \cos^2(\theta_t) \quad (16)$$

The ratio of available ranging signal power to total power is

$$\frac{P_R}{P_T} = \beta^2(\theta_r) \cdot \alpha^2(\theta_c) \cdot e^{-\theta_n^2} \cdot \cos^2(\theta_t) \quad (17)$$

The ratio of available telemetry (data) signal power to total power is

$$\frac{P_D}{P_T} = \alpha^2(\theta_r) \cdot \alpha^2(\theta_c) \cdot e^{-\theta_n^2} \cdot \sin^2(\theta_t) \quad (18)$$

In these equations, θ_r is the effective downlink ranging signal modulation index in radians rms, θ_c is the effective downlink feedthrough command signal modulation index in radians rms, θ_n is the effective noise modulation index in radians rms, and θ_t is the telemetry modulation index. If command is absent (or if, as often happens in deep space, the feedthrough command signal is small enough to be safely ignored), $\theta_c = 0$ and $\alpha(\theta_c) = 1$, so the factor representing command modulation in Equations (16), (17) and (18) is simply ignored. In Equations (16), (17) and (18), it has been assumed that the telemetry signal is bipolar (unshaped bits with squarewave subcarrier or unshaped bits directed modulating the carrier).

It is important to understand that the modulation indices θ_r , θ_c , and θ_n are *effective* modulation indices. In general, each of these effective modulation indices is less than the *design* value of the downlink ranging modulation index. The indices θ_r , θ_c , and θ_n are *not* constant; instead, they depend on signal and noise levels in the ranging channel. The equations

needed to calculate θ_r , θ_c , and θ_n are different for the two different types of AGC. Both cases are considered below.

2.3.2.1.1 *AGC with Constant Root-Mean-Square Voltage*

One type of turn-around ranging channel has an AGC that enforces a constant rms voltage at the AGC output. Since an unchanging rms voltage corresponds to an unchanging power, this type of AGC is also called a power-controlled AGC. For this type of AGC, the design value of the downlink ranging modulation index may be specified in units of radians rms; this value is denoted θ_d here. θ_d is the root-mean-square deviation of the downlink carrier phase caused by signal plus noise leaving the transponder's ranging channel.

An AGC that enforces constant rms voltage (equivalently, constant power) at the AGC output is characterized by the following relationship among the modulation indices θ_r , θ_c , θ_n , and θ_d .

$$\theta_r^2 + \theta_c^2 + \theta_n^2 = \theta_d^2 \quad (19)$$

In other words, the total power in the turn-around ranging channel, which equals the ranging signal power plus the feedthrough command signal power plus the noise power in the channel bandwidth, equals a constant value. The effective downlink modulation indices are given by

$$\theta_r = \theta_d \cdot \Lambda \cdot \beta(\phi_r) \cdot \alpha(\phi_c) \quad (20)$$

$$\theta_c = \theta_d \cdot \Lambda \cdot \alpha(\phi_r) \cdot \beta(\phi_c) \quad (21)$$

$$\theta_n = \theta_d \cdot \Lambda \cdot \sigma_N \quad (22)$$

where, as before, ϕ_r is the uplink ranging modulation index in radians rms and ϕ_c is the uplink command modulation index in radians rms. The square of σ_N is the noise variance normalized by P_T ; it is given by

$$\sigma_N^2 = B_R \cdot \left(\frac{P_T}{N_0} \Big|_{U/L} \right)^{-1} \quad (23)$$

where B_R is the turn-around ranging channel (noise-equivalent) bandwidth and $P_T/N_0|_{U/L}$ is the uplink total signal power to noise spectral density ratio. The factor Λ in Eqs. (20), (21), and (22) is given by

$$\Lambda = \frac{1}{\sqrt{\beta^2(\phi_r) \cdot \alpha^2(\phi_c) + \beta^2(\phi_c) \cdot \alpha^2(\phi_r) + \sigma_N^2}} \quad (24)$$

2.3.2.1.2 *AGC with Constant Average of Absolute Value of Voltage*

A second type of turn-around ranging channel has an AGC that causes the (short-term) average of the absolute value of the AGC output to be constant. The modulation index for this type of ranging channel is typically characterized by the peak value of the phase deviation of

the downlink carrier caused by a sinewave (and no noise) in the ranging channel. This modulation index, in units of radians peak, is denoted Ψ_d here. (Ψ_d , in radians peak, equals $\pi/180$ times the modulation index in degrees peak.) The average of the absolute value of the phase deviation is $\Psi_d \cdot 2/\pi$ radians for all signal and noise levels in the ranging channel. (However, the peak phase deviation is Ψ_d radians only when a sinewave alone is present in the ranging channel; under other circumstances, the peak phase deviation will be different.)

For this type of ranging channel, there are no analytical expressions for the effective modulation indices θ_r , θ_c , and θ_n that are valid for all signal and noise levels. In general, these effective modulation indices can only be known accurately with the help of numerical techniques. However, in a typical deep space scenario, noise dominates signal in the turn-around ranging channel, since the channel bandwidth B_R is large (typically about 1.5 MHz). When noise dominates signal in the ranging channel, the following approximations may be used to estimate the effective modulation indices:

$$\theta_r = \Psi_d \cdot \sqrt{\frac{2}{\pi}} \cdot \frac{1}{\sigma_N} \cdot \beta(\phi_r) \cdot \alpha(\phi_c) \quad (25)$$

$$\theta_c = \Psi_d \cdot \sqrt{\frac{2}{\pi}} \cdot \frac{1}{\sigma_N} \cdot \alpha(\phi_r) \cdot \beta(\phi_c) \quad (26)$$

$$\theta_n = \Psi_d \cdot \sqrt{\frac{2}{\pi}} \quad (27)$$

In Eqs. (25) and (26), σ_N is the square-root of the noise variance normalized by P_T as given in Eq. (23) and the functions $\alpha(\cdot)$ and $\beta(\cdot)$ are as defined in Table 2.

2.3.2.2 *Regenerative Ranging*

A regenerative ranging channel demodulates the uplink carrier, tracks the range clock, detects the range code, and modulates a ranging signal on the downlink. A regenerative ranging channel produces a clean ranging signal, free of command feedthrough and with little noise, because this channel has a small bandwidth. (This bandwidth is orders-of-magnitude smaller than the 1.5-MHz bandwidth of the typical turn-around ranging channel.) For the purpose of calculating the distribution of power in the downlink in the case of regenerative ranging, the following equations may be used. There will, in general, be phase jitter on the downlink ranging signal that is caused by uplink thermal noise and this jitter is an error source for the two-way range measurement. This error is considered in Section 2.5.

The carrier suppression is

$$\frac{P_C}{P_T} = \alpha^2(\theta_d) \cdot \cos^2(\theta_t) \quad (28)$$

The ratio of available ranging signal power to total power is

$$\frac{P_R}{P_T} = \beta^2(\theta_d) \cdot \cos^2(\theta_t) \quad (29)$$

The ratio of available telemetry (data) signal power to total power is

$$\frac{P_D}{P_T} = \alpha^2(\theta_d) \cdot \sin^2(\theta_t) \quad (30)$$

In these equations, θ_d is the design value of the downlink ranging modulation index in radians rms, and θ_t is the telemetry modulation index.

2.4 Uplink Spectrum

The spectrum of the uplink carrier is of some concern because of the very large transmitter powers used on the uplink for deep space missions. A mathematical model for this spectrum is given here for the case of a sinewave range clock and no command.

A PN ranging signal is periodic, so its spectrum consists of discrete spectral lines. The spectrum of an uplink carrier that has been phase modulated by only a PN ranging signal also consists of discrete spectral lines.

As described in Section 2.2, the composite chip sequence $c'(\cdot)$ is similar to the range clock $c_1'(\cdot)$, except that some chips are inverted. A discrepancy signal $d'(\cdot)$ is defined by

$$d'(i) = c_1'(i) \cdot c'(i) \quad (31)$$

$d'(i)$ equals +1 when the range clock and the composite code agree, which is most of the time. When the range clock and the composite code disagree, $d'(i)$ equals -1. The PN ranging signal may be mathematically modeled as $d(i)\sin(\pi t/T_c)$ for $iT_c \leq t < (i+1)T_c$, where T_c is the chip period. In words, the PN ranging signal is a sinewave (range clock) of frequency $1/(2T_c)$ except that there is an occasional inversion of a half-cycle. When this signal phase modulates the uplink carrier with modulation index ϕ_r (radians rms), the fractional power in each discrete spectral line is given by

$$\frac{P_k}{P_T} = |X_k|^2 = \begin{cases} \text{fraction of uplink total power in the} \\ \text{discrete spectral line with frequency} \\ f_c + \frac{k}{LT_c} \end{cases} \quad (32)$$

where P_T is the total uplink power, f_c is the uplink carrier frequency, L is the period in chips of the composite code, k is an integer harmonic number, and X_k is given by

$$X_k = \frac{1}{L} \sum_{m=-\infty}^{\infty} \text{sinc}\left(\frac{m}{2} - \frac{k}{L}\right) \sum_{n=0}^{L-1} J_m(\sqrt{2} \phi_r d'(n)) \exp\left[j\pi\left(n + \frac{1}{2}\right)\left(m - \frac{2k}{L}\right)\right] \quad (33)$$

where $J_m(\cdot)$ is the Bessel function of the first kind of order m , and

$$\text{sinc}(x) = \frac{\sin(\pi x)}{\pi x} \quad (34)$$

Equation (33) may be evaluated numerically. The values of the Bessel functions decrease very rapidly with increasing $|m|$, so in practice it is possible to get good accuracy while including only a few terms from the sum over the integer m . In evaluating Equation (33), the following identity is useful.

$$J_{-m}(x) = \begin{cases} J_m(x), & m \text{ even} \\ -J_m(x), & m \text{ odd} \end{cases} \quad (35)$$

There is a symmetrical power distribution about the carrier. So for every discrete spectral line at $f_c + k/(LT)$ whose power is given by Equation (32), there is also a discrete spectral line at $f_c - k/(LT)$ with the same power.

Figure 3 illustrates the uplink spectrum for a sinewave range clock with the JPL PN code and a modulation index $\phi_r = 0.2$ rad rms. The tallest spectral line is the residual carrier with a carrier suppression of -0.2 dB. The next tallest spectral lines are located at $f_c - f_{RC}$ and $f_c + f_{RC}$, where $f_{RC} = 1/(2T_c)$ is the range-clock frequency; these spectral lines each have a power of -17.5 dB relative to P_T , which was found by using $k = L/2$ in Equation (32). At each of the frequencies $f_c - 2f_{RC}$ and $f_c + 2f_{RC}$ there is a power of -39.7 dB relative to P_T (found with $k = L$). The smaller spectral lines that lie between $f_c - 2f_{RC}$ and $f_c + 2f_{RC}$ are due to the occasional inversions of half-cycles as represented by $d'(i)$.

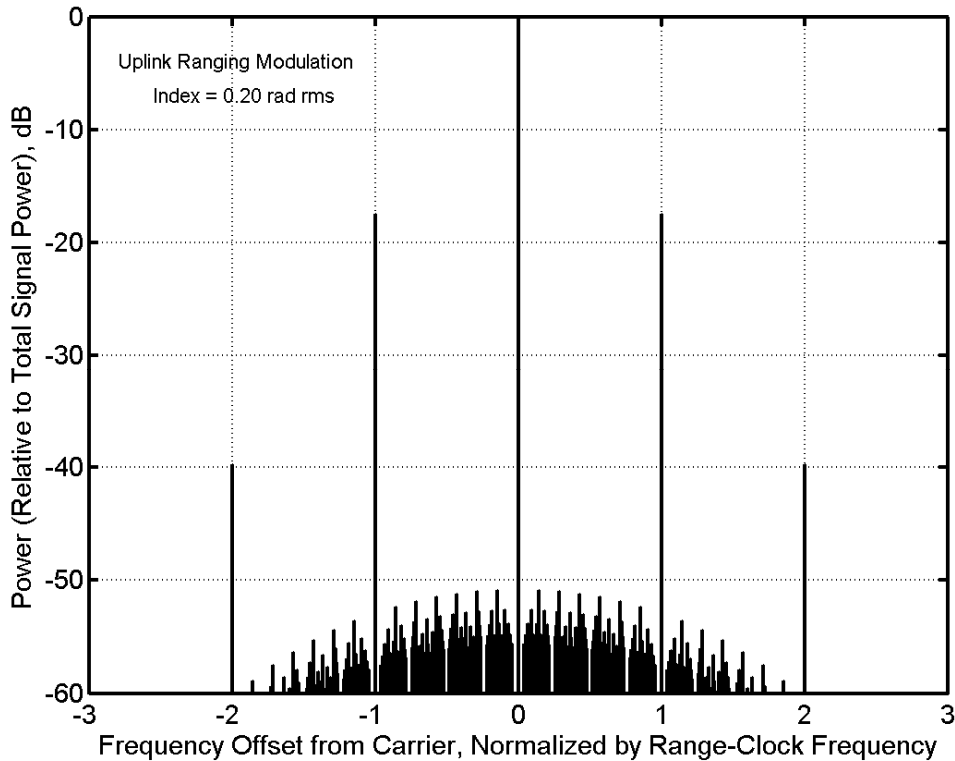


Figure 3. Uplink Spectrum for the JPL PN Code Ranging Signal

The representation of the uplink spectrum in the above analysis is approximate. If more accurate results are required, it is necessary to take into account the presence of the uplink ranging filter that filters the ranging signal going to the modulator. The filter has the frequency response shown in Figure 4 and is inserted between the URA and the exciter. This filter constrains the spectrum of the baseband ranging signal, thereby reducing the bandwidth of the modulated carrier, for the sake of spectral compliance. A more accurate determination of the uplink spectrum, one that accounts for the uplink ranging filter, would probably have to be done with a simulation.

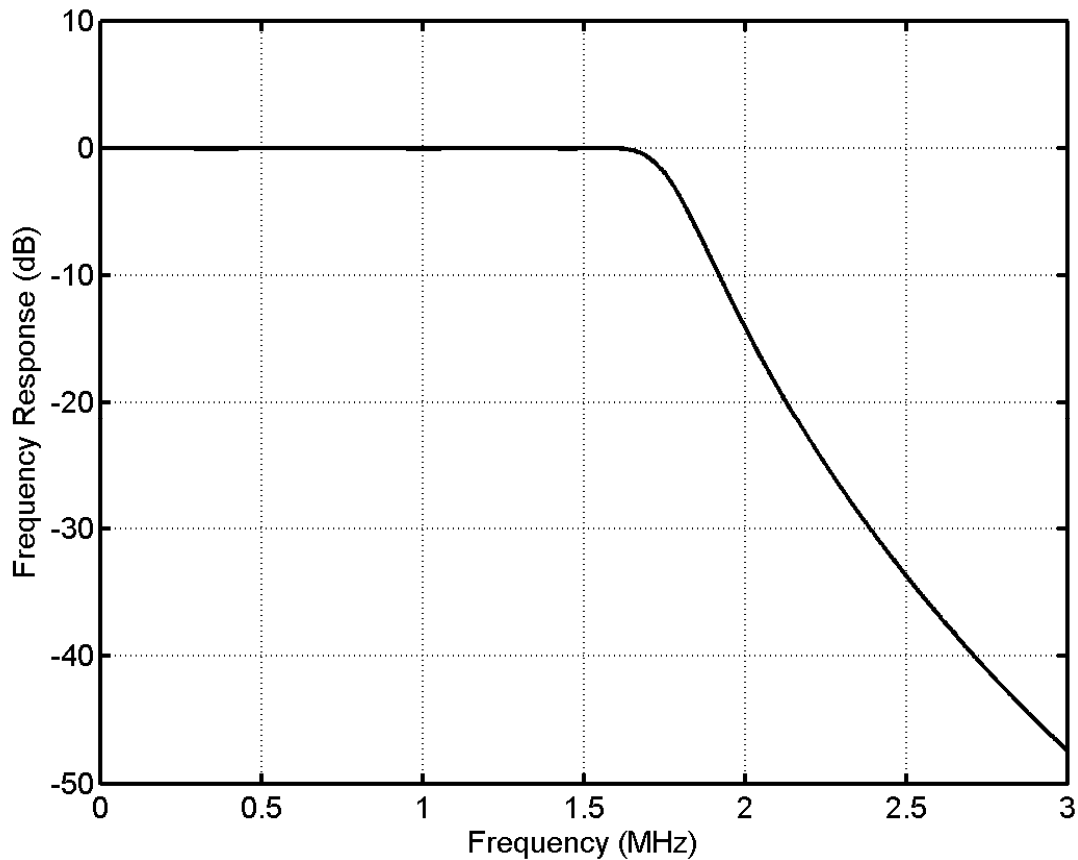


Figure 4. Uplink Ranging Filter Frequency Response

2.5 *Range Measurement Performance*

Thermal noise has two effects on range measurements. First, there is a standard deviation of the range measurement error due to thermal noise. Second, there is a probability of acquisition of the range measurement that is less than 100% due to the presence of thermal noise. The cross-correlation factors of a composite code plays a role in the performance of PN ranging in the presence of thermal noise.

2.5.1 Cross-Correlation Factors

The cross-correlation factors R_n (with zero delay) are defined by

$$R_n = \frac{1}{L} \sum_{i=0}^{L-1} c'(i)c_n'(i) \quad (36)$$

where L is the period (in chips) of the composite code, $c'(i) = \pm 1$ is the chip sequence, and $c_n'(i) = \pm 1$ is the (periodic extension of the) chip sequence for the n -th component code. The cross-correlation factors are given in tables that follow: Table 3 for the JPL PN code, Table 4 for the T4B code, and Table 5 for the T2B code.

Table 3. Cross-Correlation Factors, JPL PN Code

n	λ_n	R_n
1	2	0.9544
2	7	0.0456
3	11	0.0456
4	15	0.0456
5	19	0.0456
6	23	0.0456

Table 4. Cross-Correlation Factors, T4B (Reference 5)

n	λ_n	R_n
1	2	0.9387
2	7	0.0613
3	11	0.0613
4	15	0.0613
5	19	0.0613
6	23	0.0613

Table 5. Cross-Correlation Factors, T2B (Reference 5)

n	λ_n	R_n
1	2	0.6274
2	7	0.2447
3	11	0.2481
4	15	0.2490
5	19	0.2492
6	23	0.2496

2.5.2 Range Measurement Error Due to Thermal Noise

The standard deviation of range measurement error σ_ρ , in meters rms (one way), due to downlink thermal noise is given by

$$\sigma_\rho = \begin{cases} \frac{c}{f_{RC} \cdot A_c \cdot R_1 \cdot \sqrt{32\pi^2 \cdot T \cdot (P_R/N_0)}}, & \text{sinewave range clock} \\ \frac{c}{f_{RC} \cdot A_c \cdot R_1 \cdot \sqrt{256 \cdot T \cdot (P_R/N_0)}}, & \text{squarewave range clock} \end{cases} \quad (37)$$

where

c = speed of electromagnetic waves in vacuum, 3.0×10^8 m/s

A_c = fractional loss of correlation amplitude due to frequency mismatch ($A_c \leq 1$)

R_1 = cross-correlation factor for the correlation against the range clock

T = range measurement integration time

f_{RC} = frequency of the range clock

$A_c = 1$ under the normal circumstances where on the downlink the range clock is coherently related to the carrier. In the special case of non-coherent ranging, $A_c < 1$.

P_R/N_0 , the ratio of the downlink ranging signal power to the noise spectral density, is given by

$$\frac{P_R}{N_0} = \frac{P_R}{P_T} \cdot \frac{P_T}{N_0} \Big|_{D/L} \quad (38)$$

where $P_T/N_0|_{D/L}$ is the downlink total signal to noise spectral density ratio and where P_R/P_T is the ratio of downlink ranging signal power to total power as given by Equation (17) for turn-around (non-regenerative) ranging or as given by Equation (29) for regenerative ranging. In the case of turn-around ranging, uplink thermal noise has an effect on measurement error through its effect on P_R/P_T , which is calculated using Equation (17).

The standard deviation of the two-way time delay σ_τ , in seconds, is related to σ_ρ , as given in Eq. (37), by

$$\sigma_\tau = \frac{2}{c} \cdot \sigma_\rho \quad (39)$$

The factor of 2 in Eq. (39) accounts for the fact that σ_ρ characterizes the error in the *one*-way range, while σ_τ characterizes the error in a *two*-way time delay. The standard deviation of the two-way phase delay σ_{RU} , as measured in range units, is related to σ_τ by

$$\sigma_{RU} = \begin{cases} \frac{f_S}{2} \cdot \sigma_\tau, & \text{S-band uplink} \\ \frac{221}{749} \cdot \frac{f_X}{2} \cdot \sigma_\tau, & \text{X-band uplink} \end{cases} \quad (40)$$

where f_S is the frequency of an S-band uplink carrier, and f_X is the frequency of an X-band uplink carrier.

In the case of regenerative ranging, uplink thermal noise leads to phase jitter on the regenerated ranging signal. This phase jitter arises in the tracking loop that is part of the regeneration signal processing (Reference 6). This tracking jitter is a potential error source for the two-way range measurement. The standard deviation $\sigma_{U/L}$ of range measurement error (meters rms, one way) for this error source is given by

$$\sigma_{U/L} = \begin{cases} \frac{c}{4\pi R_1 f_{RC}} \sqrt{\frac{B_{RL}}{P_R/N_0|_{U/L}}}, & \text{sinewave range clock} \\ \frac{c}{8R_1 f_{RC}} \sqrt{\frac{B_{RL}}{P_R/N_0|_{U/L}}}, & \text{squarewave range clock} \end{cases} \quad (41)$$

where B_{RL} is the bandwidth of the loop that tracks the uplink range clock and $P_R/N_0|_{U/L}$ is the uplink signal power to noise spectral density ratio. This error only applies in the case of regenerative ranging.

Regenerative ranging has better performance than turn-around ranging. A difference in bandwidth is the reason for this. With regenerative ranging, the bandwidth of the transponder's range-clock loop, B_{RL} in Equation (41), is typically small, perhaps a few hertz. With turn-around ranging, the bandwidth of the transponder's filter, B_R in Equation (23), is typically about 1.5 MHz.

For the JPL and T4B codes, the standard deviation of range measurement error (meters) due to thermal noise is plotted in Figure 5 against the product $T \cdot (P_R/N_0)$, expressed in

decibels: $10 \log(T \cdot P_R/N_0)$. These curves were calculated from Equation (37) using the cross-correlation factor R_1 given in Table 3 for the JPL code and Table 4 for the T4B code. Also, the range clock was taken to be a 1-MHz sinewave and A_c was taken to be 1.

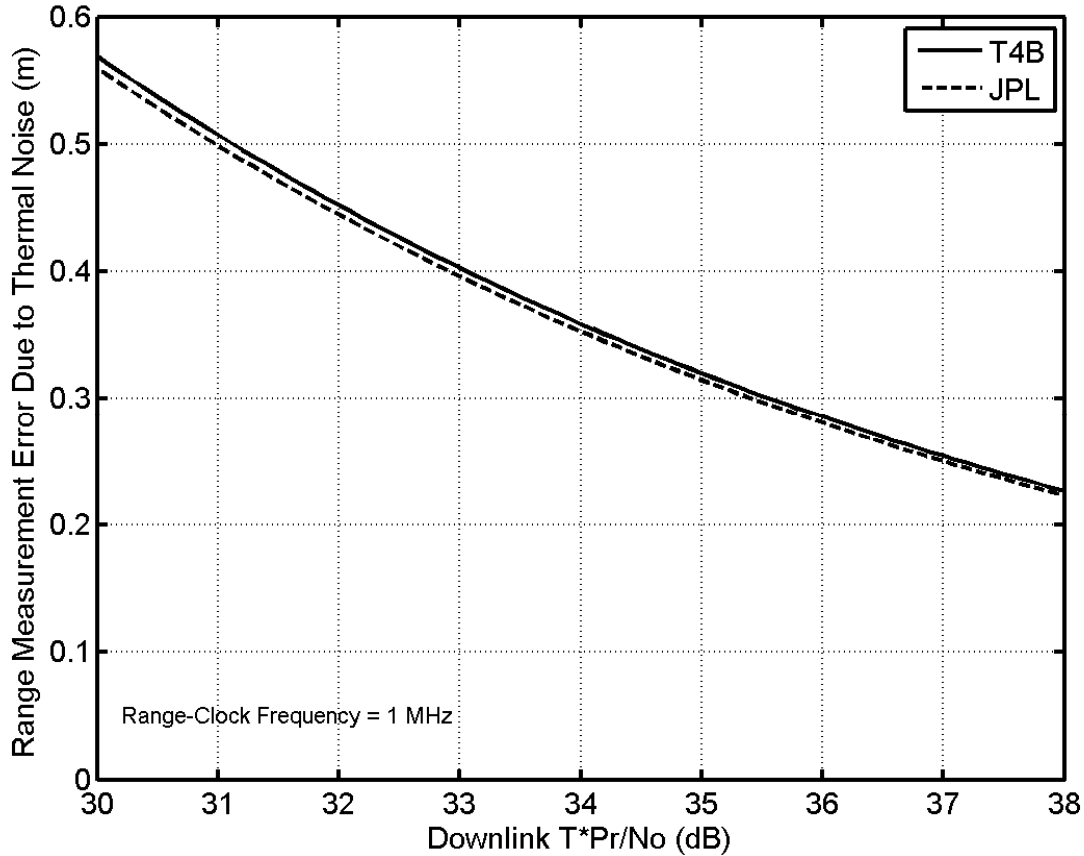


Figure 5. Standard Deviation of Range Measurement Error for the JPL and T4B Codes

The T2B code was designed to operate at smaller values of $T \cdot (P_R/N_0)$. For the T2B code, the standard deviation of range measurement error (meters) due to thermal noise is plotted in Figure 6. This curve was calculated from Equation (37) using the cross-correlation factor R_1 given in Table 5. The range clock was taken to be a 1-MHz sinewave and A_c was taken to be 1.

The ratio P_R/N_0 is defined for the downlink, but for turn-around ranging it accounts for the uplink thermal noise as well. P_R/N_0 is calculated from P_R/P_T , which depends on the *effective* downlink ranging modulation index θ_r , a function of the signal-to-noise ratio in the transponder's ranging channel.

In the case of regenerative ranging, Figure 5 and Figure 6 do not account for the uplink thermal noise. The signal-to-noise ratio in the transponder's range-clock loop contributes an error to the two-way range measurement that needs to be accounted separately, by means of

Equation (41). However, the error $\sigma_{U/L}$ of Equation (41) is often small compared with the σ_ρ of Equation (37).

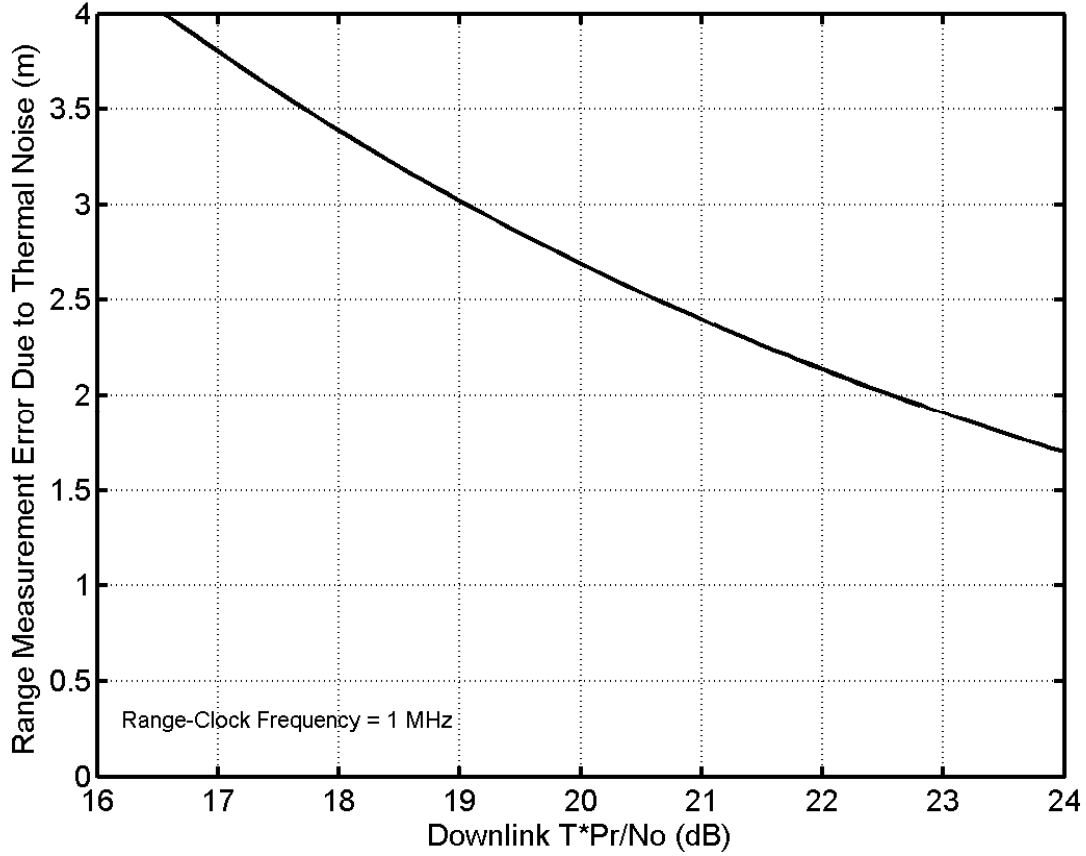


Figure 6. Standard Deviation of Range Measurement Error for the T2B Code

2.5.3 Probability of Acquisition

The probability of acquisition is, for the case of N components, given by

$$P_{\text{acq}} = \prod_{n=2}^N P_n \quad (42)$$

where P_n is the probability of acquiring the n -th component code ($2 \leq n \leq N$). For the JPL PN code, the T4B code and the T2B code, $N = 6$. Each P_n is calculated by

$$P_n = \frac{1}{\sqrt{\pi}} \int_{-\infty}^{\infty} e^{-x^2} \left(\frac{1 + \text{erf}(x + A_c R_n \sqrt{T \cdot (P_R/N_0)})}{2} \right)^{\lambda_n - 1} dx \quad (43)$$

where λ_n and R_n are the code length (in chips) and cross-correlation factor for the n -th component code. Numerical integration is required to evaluate Equation (43). The error function $\text{erf}(\cdot)$ is defined by

$$\text{erf}(y) = \frac{2}{\sqrt{\pi}} \int_0^y e^{-t^2} dt \quad (44)$$

Equations (37) and (43) are based on the assumption that the local model of the range clock has a wave shape that matches that of the received range clock. In other words, when the downlink range clock is sinewave, the local model of the range clock used in the correlation is assumed likewise to be sinewave; and when the downlink range clock is squarewave, the local model of the range clock used in the correlation is assumed likewise to be squarewave.

Table 6 lists required values for $(A_c R_n)^2 \cdot T \cdot P_R/N_0$ (in decibels) as a function of λ_n (the code length) and P_n (the probability of acquiring the n -th component code). This table is based on Equation (43). Here is an example of how this table can be used. If the desired P_n for a component code of length 19 is 0.95, then $\log(P_n) = -0.022$. From Table 6, the decibel values 7.9 dB and 8.5 dB are found for $\log(P_n) = -0.030$ and $\log(P_n) = -0.020$, respectively. An interpolation suggests that $(A_c R_n)^2 \cdot T \cdot P_R/N_0$ must be about 8.4 dB for a $P_n = 0.95$. Of course, it is important to recall that $P_n = 0.95$ is not the probability of acquisition of the composite code. There are several component codes that must be acquired before acquisition of the composite code is complete. P_{acq} is given by Equation (42), and it will be less than the value of any individual P_n . The value that Equation (42) gives for P_{acq} is, in general, between 0 and 1. P_{acq} is often characterized as a percentage (between 0% and 100%).

P_{acq} is plotted in Figure 7 and Figure 8 against the product $T \cdot (P_R/N_0)$, in decibels: $10 \log(T \cdot P_R/N_0)$. Figure 7 has a curve for the JPL PN code and one for the T4B code. Figure 8 has the curve for the T2B code. These curves were calculated from Equations (42) and (43) using $A_c = 1$ and cross-correlation factors from Table 3, Table 4, and Table 5.

An approximation of P_{acq} may be calculated using the following curve fit:

$$P_{\text{acq}} = \begin{cases} c_3 Z^3 + c_2 Z^2 + c_1 Z + c_0, & Z_1 \leq Z \leq Z_2 \\ 1.00, & Z > Z_2 \end{cases} \quad (45)$$

where Z is the product $T \cdot (P_R/N_0)$ in units of decibels,

$$Z = 10 \log[T \cdot (P_R/N_0)] \quad \text{dB} \quad (46)$$

The parameters for the model of Equation (45) are given in Table 7. The correct set of parameters depends on the code (JPL PN, T4B, or T2B), as indicated in Table 7. The model of Equation (45) is not reliable for $Z < Z_1$ dB. For $Z > Z_2$ dB, the approximation $P_{\text{acq}} = 1$ may be used.

Table 6. Required $(A_c R_n)^2 \cdot T \cdot P_R / N_0$ (in decibels) for Given λ_n and P_n

$\log(P_n)$	$\lambda_n = 7$	$\lambda_n = 11$	$\lambda_n = 15$	$\lambda_n = 19$	$\lambda_n = 23$
-0.050	5.7	6.5	6.9	7.1	7.4
-0.040	6.2	6.9	7.2	7.5	7.7
-0.030	6.7	7.3	7.7	7.9	8.1
-0.020	7.4	7.9	8.3	8.5	8.7
-0.010	8.3	8.8	9.1	9.3	9.4
-0.009	8.4	8.9	9.2	9.4	9.5
-0.008	8.6	9.0	9.3	9.5	9.7
-0.007	8.7	9.2	9.4	9.6	9.8
-0.006	8.9	9.3	9.6	9.8	9.9
-0.005	9.1	9.5	9.8	9.9	10.1
-0.004	9.3	9.7	10.0	10.1	10.3
-0.003	9.6	10.0	10.2	10.4	10.5
-0.002	9.9	10.3	10.5	10.7	10.8
-0.001	10.5	10.8	11.0	11.1	11.3

Table 7. Parameters for Equation (45)

	JPL PN	T4B	T2B
Z_1	30 dB	28 dB	16 dB
Z_2	37 dB	35 dB	23 dB
c_3	-0.0039916	-0.0038441	-0.0037013
c_2	0.400534	0.356736	0.208431
c_1	-13.2253	-10.8645	-3.7427
c_0	144.154	109.048	21.833

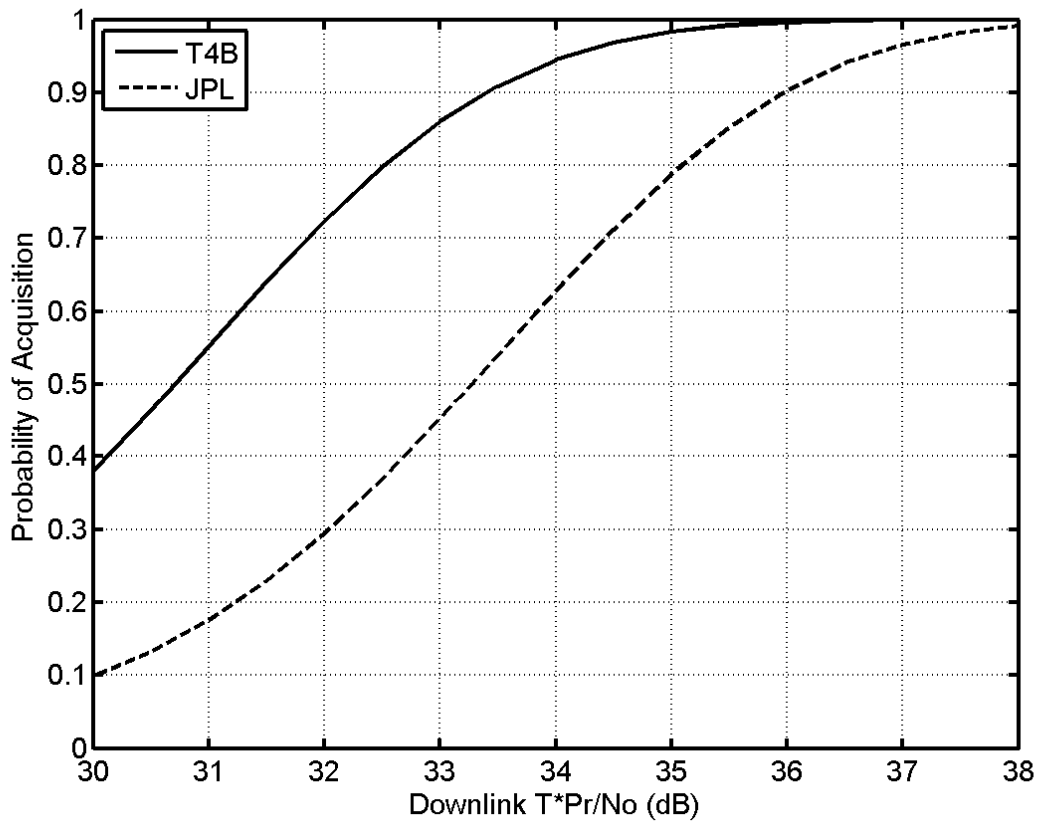


Figure 7. Probability of Acquisition for the JPL PN Code and the T4B Code

Comparing Figure 5 and Figure 7, it becomes clear that the JPL PN code was designed to give a range measurement error (due to thermal noise) of about 0.2 to 0.3 meter when the product $T \cdot P_R / N_0$ is just large enough (about 37 to 38 dB) to assure a high probability of acquisition. The T4B code has better acquisition performance than the JPL PN code. The range measurement error is about the same for the JPL PN code and the T4B code. The T2B code achieves a high P_{acq} for considerably smaller $T \cdot P_R / N_0$, but the price is a larger standard deviation of range measurement error (Reference 3).

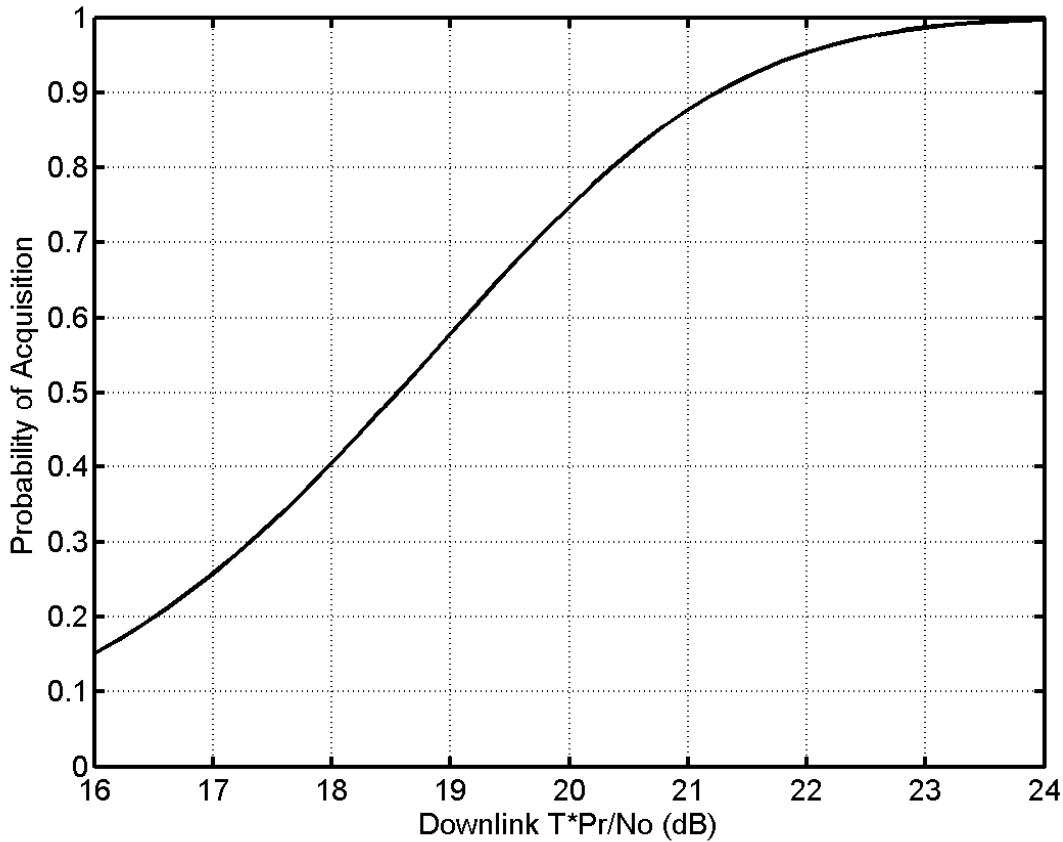


Figure 8. Probability of Acquisition for the T2B Code

2.5.4 *Processing a Set of Range Measurements*

For a given PN range code, a minimum $T \cdot (P_R/N_0)$ product is needed to achieve a high P_{acq} , and there is an approximate range measurement error (standard deviation) corresponding to this $T \cdot (P_R/N_0)$. In the example discussed above, the JPL PN code ordinarily requires that $T \cdot (P_R/N_0)$ be about 37 to 38 dB in order to assure a high P_{acq} , and the corresponding range measurement error is about 0.2 to 0.3 meter.

Sometimes the available $T \cdot (P_R/N_0)$ is smaller than the minimum value for which a range code was designed to work. It is still possible to acquire range measurements with the correct resolution of the ambiguity even under the circumstance of a low $T \cdot (P_R/N_0)$. This is accomplished by using a large set of range measurements (obtained from one station tracking one spacecraft).

Reference 7 describes the “Plurality Voting Method” for accomplishing range acquisitions for a large measurement data set when $T \cdot (P_R/N_0)$ is low. This method employs range residuals for the given set of range measurements. A range residual is the difference between the measured two-way delay and the predicted two-way delay, where the predicted value is computed from a spacecraft ephemeris. Doppler velocity residuals can also be used. The Plurality Voting Method, making use of a large set of range measurements, increases the

acquisition probability beyond that given in Eq. (42). This method does not, however, improve the standard deviation of acquired range measurements. The Plurality Voting Method has value in scenarios where $T \cdot (P_R/N_0)$ is adequate for the required range accuracy (standard deviation) but is inadequate (in the absence of this special method) for the required acquisition probability.

2.5.5 *Comparison of PN Ranging and Sequential Ranging*

It is instructive to compare the performance of turn-around PN ranging with sequential ranging (Reference 8). For both techniques, a minimum integration time T can be calculated as a function of P_R/N_0 for a given range measurement error σ_ρ (due to thermal noise) and a given P_{acq} . For the purpose of the present comparison, σ_ρ is taken to be 0.2 m and P_{acq} is taken to be 0.99. Furthermore, the range-clock frequency f_{RC} is taken to be 1 MHz.

For the analysis presented here, the minimum T is calculated for the JPL PN code by finding, for a given P_R/N_0 , the smallest T that satisfies the two constraints: $\sigma_\rho < 0.2$ m, as calculated with Equation (37), and $P_{\text{acq}} > 0.99$, as calculated with Equations (42) and (43).

For sequential ranging, the number of sinewaves in the sequence is taken to be 20; this gives an ambiguity resolution of 78,590 km, comparable with the 75,660 km ambiguity resolution offered by the JPL PN code. The minimum T for sequential ranging is the minimum cycle time consistent with a range error (due to thermal noise) of 0.2 m and a probability of acquisition of 0.99. The cycle time includes the range-clock integration time T_1 plus 19 times the ambiguity integration time T_2 plus the required deadtime seconds.

Figure 9 shows the ratio of the minimum T (cycle time) for sequential ranging to the minimum T (integration time) for PN ranging as a function of P_R/N_0 . This figure is intended as a performance comparison of sequential ranging and turn-around PN ranging. The underlying assumption is that P_R/N_0 is approximately the same for these two ranging techniques for a given set of link parameters.

In principle, a plot like this also applies to regenerative PN ranging. However, P_R/N_0 will not be the same for regenerative PN ranging and (non-regenerative) sequential ranging. In general, it is expected that regenerative PN ranging will out-perform (non-regenerative) sequential ranging.

The results of Figure 9 suggest that sequential ranging has a small performance advantage over turn-around PN ranging for small P_R/N_0 (less than about 12 dB-Hz for the parameters used here) but that PN ranging has a performance advantage for P_R/N_0 larger than this. When the sequential ranging minimum T is larger than the PN ranging minimum T (that is, when P_R/N_0 is larger than about 12 dB-Hz), the choice to use PN ranging means that more range measurements can be made in a given period than can be made with sequential ranging.

PN ranging has an operational advantage over sequential ranging. With sequential ranging, a large increase in the RTLT during the tracking pass forces a measurement restart. This is not an issue for PN ranging. The PN range code has a period of approximately 0.5 second when the range clock has its typical frequency of about 1 MHz. (The measurement integration time T is larger, as the measurement comprises multiple periods of the PN range code.) With PN ranging, the downlink can start processing at any 1-second boundary.

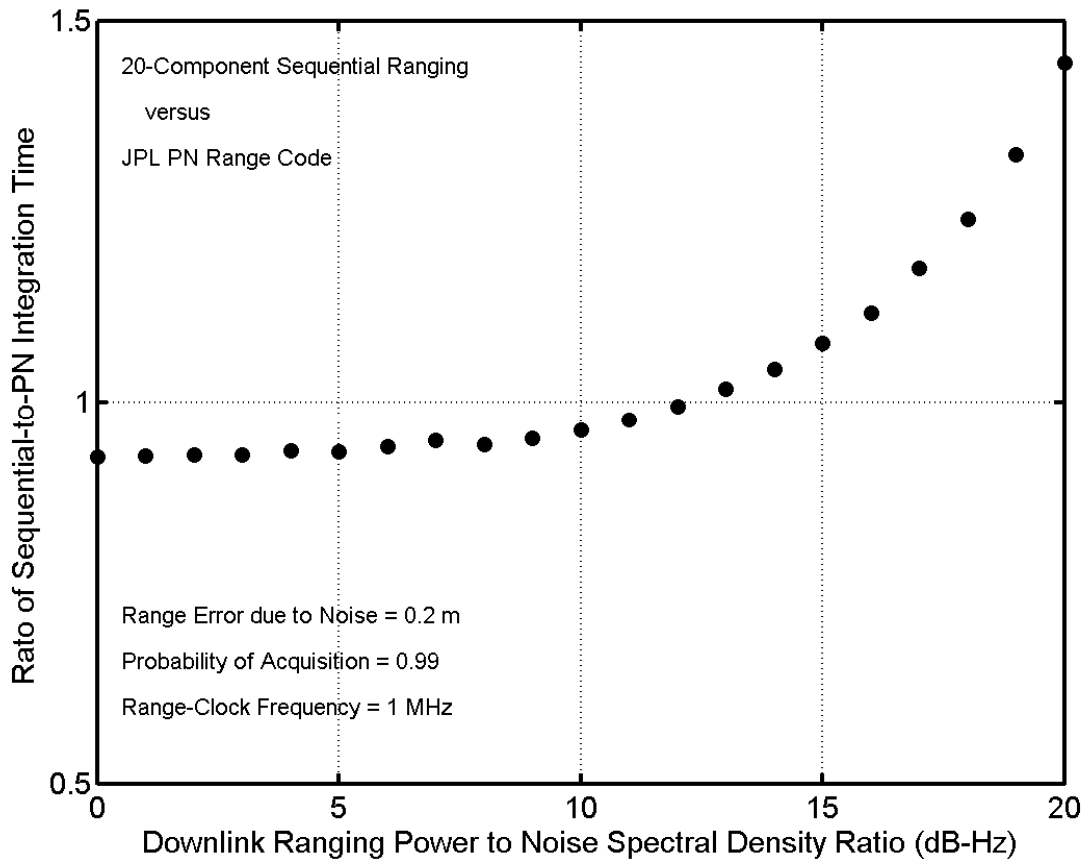


Figure 9. Comparison of Sequential Ranging and PN Ranging

2.5.6 *Non-Coherent Operation*

A non-coherent ranging technique has been described in Reference 9. For the sake of economy, this technique employs a transceiver, rather than a transponder, at the spacecraft. With such a technique, the downlink carrier is not coherent with the uplink carrier, and the downlink range clock is not coherent with the downlink carrier. This means that there will ordinarily be a frequency mismatch between the received downlink range clock and its local model. This mismatch is to be minimized by Doppler compensation of the uplink carrier, but it will not be possible, in general, to eliminate completely the frequency mismatch. With this non-coherent technique, range measurement performance will not be as good as that which can be achieved with coherent operation using a transponder. Nonetheless, non-coherent range measurement performance is expected to be adequate for some mission scenarios.

The frequency mismatch inherent in non-coherent ranging has two effects on performance. One is a loss A_c of correlation amplitude, which increases the thermal noise contribution to measurement error. The other is a direct contribution to range measurement error. This direct contribution is much the more important of these two effects.

The loss of correlation amplitude is represented by A_c where $0 < A_c < 1$. The standard deviation σ_ρ of range measurement error due to thermal noise is given by Equation (37), and the probability of acquisition (considering the effect of thermal noise) is given by Equations (42) and (43). The amplitude loss factor A_c is, for non-coherent operation, given by

$$A_c = |\text{sinc}(2\Delta f_{RC}T)| \quad (47)$$

where Δf_{RC} is the frequency mismatch between the received range clock and its local model. The function $\text{sinc}(\cdot)$ is defined by Equation (34). For coherent operation, $\Delta f_{RC} = 0$ and $A_c = 1$.

The direct contribution of frequency mismatch to range measurement error is given by

$$\text{range error due to } \Delta f_{RC} = \frac{c}{4} \cdot \frac{\Delta f_{RC}}{f_{RC}} \cdot T, \quad \text{m} \quad (48)$$

The range error given by Eq. (48) is in meters (with c in m/s, T in seconds, and with Δf_{RC} and f_{RC} in the same units). It is worth noting that this measurement error is directly proportional to both the fractional frequency mismatch $\Delta f_{RC}/f_{RC}$ and the measurement integration time T . The fractional frequency error will, in general, comprise two terms: a fractional frequency error due to uncertainty in the spacecraft oscillator frequency and a fractional frequency error due to imperfect uplink Doppler predicts.

Non-coherent ranging measurements should be done with regenerative ranging using PN signals. The reason for this follows. The direct error contribution due to frequency mismatch is directly proportional to the measurement integration time, as can be seen in Equation (48). So, for non-coherent operation, it is important to make T as small as possible. This is achieved with regenerative ranging, and regenerative ranging is only available with a PN ranging signal.

With non-coherent operation, the range error due to frequency mismatch increases with T and the range error due to thermal noise decreases with T . Therefore, it is important to seek an optimal value for T , in order to get the best possible performance. Reference 9 offers guidance in this matter.

2.6 *Range Corrections*

Range is defined to be the distance from the reference point on the DSS antenna to the reference point on the spacecraft antenna. The reference point of a DSS antenna is the intersection of the azimuth and elevation axes. When the two-way time delay is measured, the result includes more than just the two-way delay between the reference points of the DSS and spacecraft antennas. The measured two-way delay also includes station delay and spacecraft delay. These extra delays must be determined through calibration and then removed from the measured two-way time delay. The station delay is determined in two parts: the DSS delay and the Z-correction.

Before correction of the station delay, a range measurement provides the two-way delay through the station uplink path, starting from the URA, to and from the spacecraft, and through the station downlink path, ending in the RRT. Figure 10 shows the equipment configuration at the station when both uplink and downlink are in a common band. It is

necessary to determine the uplink station delay for the path from the URA to the antenna reference point, to determine the downlink station delay for the path from the antenna reference point to the RRT, and to remove these delays from the measured two-way delay.

2.6.1 DSS Delay

The DSS delay is obtained by a calibration that mimics an actual two-way range measurement, except that the signal path lies entirely within the station. A sample of the uplink carrier is diverted through a coupler to a test translator. The test translator shifts the carrier to the downlink frequency (while not altering the modulation) and feeds this frequency-shifted carrier to a coupler that places it on the downlink path within the station. The DSS delay contains most of the station delay. To be precise, the DSS delay comprises the delay from the URA to the ranging coupler on the uplink, the delay through the test translator (and its cables), and the delay from the ranging coupler on the downlink to the RRT. When the uplink and downlink are in a common band, Figure 10 shows the configuration. When the uplink and downlink are in different bands, Figure 11 shows the configuration.

The DSS delay is station and configuration dependent. It should be measured for every ranging pass. This measurement is called precal for pre-track calibration and postcal for post-track calibration. The former is done at the beginning of a ranging pass; the latter is only needed when there is a change in equipment configuration during the track or precal was not performed due to a lack of time.

2.6.2 Z-Correction

The DSS delay itself must be corrected. This is accomplished with the Z-correction. The DSS delay includes the delay through the test translator (and its cables), but the test translator is not in the signal path of an actual range measurement. Moreover, the DSS delay does not include, but should include, the delays between the ranging couplers and the antenna reference point.

The Z-correction is defined as the delay through the test translator (and its cables) minus the uplink and downlink delays between the ranging couplers and the antenna reference point. The DSS delay minus the Z-correction therefore gives the delay between the URA and the antenna reference point plus the delay between the antenna reference point and the RRT. This is exactly the quantity that must be subtracted from a range measurement in order to produce a two-way delay relative to the antenna reference point.

The test translator delay is measured by installing a zero delay device (ZDD) in place of the test translator. Since the ZDD delay is measured in the laboratory, the signal delay contributed by the test translator can be calculated to a known precision. This measurement is made approximately once each year or when there are hardware changes in this portion of the signal path. The delays between the ranging couplers and the antenna reference point are stable and need not be updated often; they are determined by a combination of calculation and measurement.

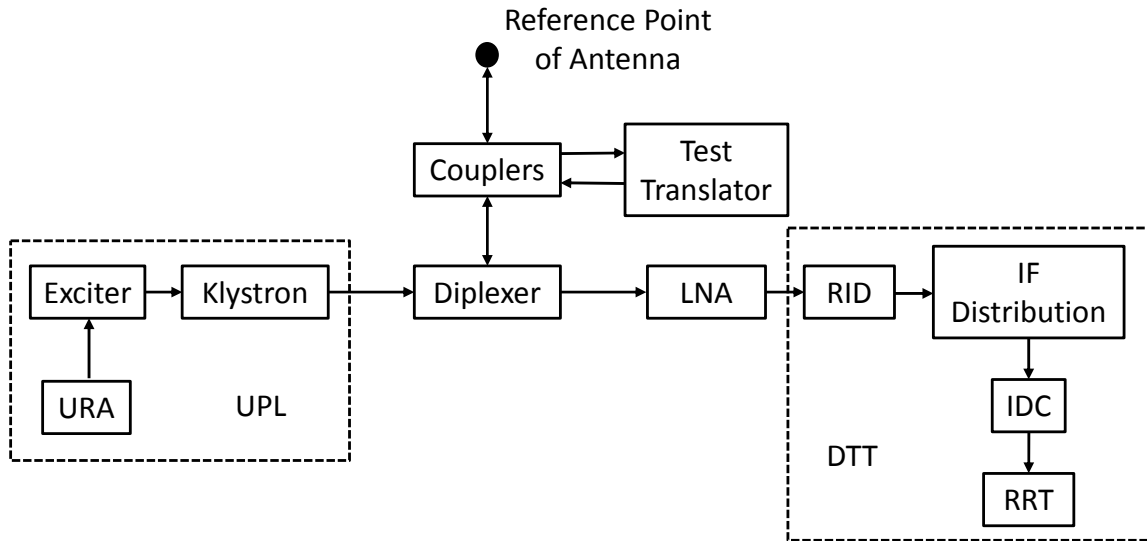


Figure 10. DSS Delay Calibration, Uplink and Downlink in a Common Band

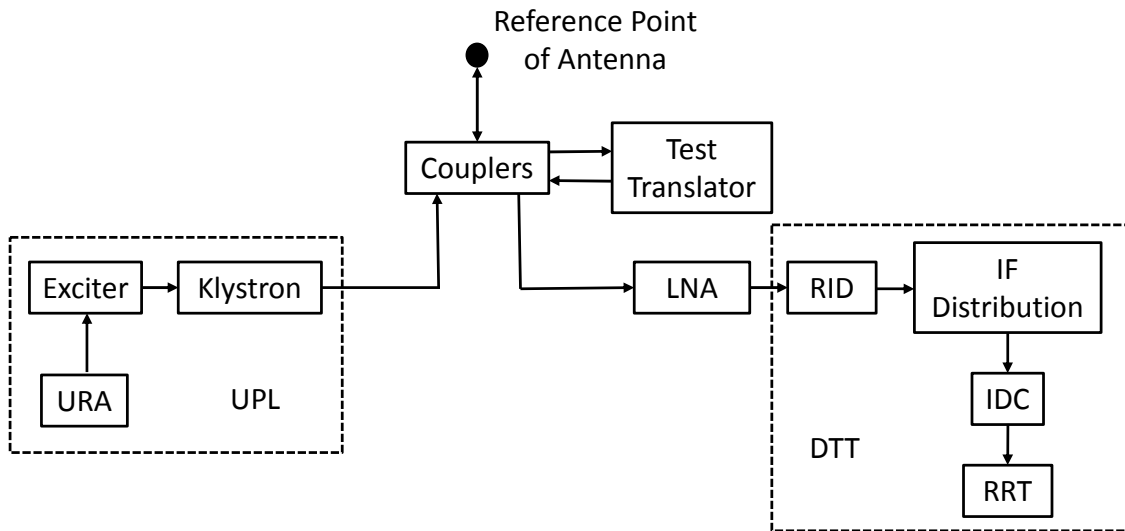


Figure 11. DSS Delay Calibration, Uplink and Downlink in Different Bands

2.7 *Total Error for Range Measurement*

Several error sources contribute to the total error for a range measurement. For two-way range measurement, the two most important error sources are typically thermal noise and station calibration error. The error due to thermal noise is discussed in Section 2.5. The

error in calibrating and removing the station delay is often the dominant error source for two-way ranging. For two-way range measurements in the X band, there is typically about 6 ns of station calibration error in the two-way delay, corresponding to a (one-way) range error of about 1 meter.

The error in calibrating and removing the spacecraft delay is stable for a given spacecraft and a given band pairing (for example, X band on the uplink and X band on the downlink). The orbit determination program can, given enough range measurements for this spacecraft and band pairing, solve for this error.

There are error contributions, usually small compared to the station calibration error, due to the passage of the uplink and downlink through the troposphere, ionosphere and solar corona (Reference 10). When the angle between the sun and the spacecraft, as seen from the station, is small and the spacecraft is beyond the sun, the error contribution from the solar corona can become the dominant contributor to error in the range measurement.

For three-way ranging (in which one station transmits the uplink and a second station receives the downlink), the total delay measurement error is larger than for two-way. There are two reasons for this. First, there is a clock offset between the transmitting and receiving stations. Second, the calibration of the station delays is more difficult to achieve accurately in this case.

References

1. J. B. Berner, S. H. Bryant, and P. W. Kinman, "Range Measurement as Practiced in the Deep Space Network," *Proceedings of the IEEE*, Vol. 95, No. 11, November 2007.
2. J. B. Berner and S. H. Bryant, "New Tracking Implementation in the Deep Space Network," *2nd ESA Workshop on Tracking, Telemetry and Command Systems for Space Applications*, October 29-31, 2001, Noordwijk, The Netherlands.
3. Consultative Committee for Space Data Systems, "Pseudo-Noise (PN) Ranging Systems," *CCSDS 414.1-B-2*, February 2014.
4. P. W. Kinman and J. B. Berner, "Two-Way Ranging During Early Mission Phase," *2003 IEEE Aerospace Conference*, March 8-15, 2003, Big Sky, MT.
5. J. L. Massey, G. Boscagli, and E. Vassallo, "Regenerative Pseudo-Noise (PN) Ranging Sequences for Deep-Space Missions," *Int. J. Satellite Communications and Networking*, Vol. 25, No. 3, pp. 285-304, May/June 2007.
6. J. B. Berner, J. M. Layland, P. W. Kinman, and J. R. Smith, "Regenerative Pseudo-Noise Ranging for Deep-Space Applications," *TMO Progress Report 42-137*, Jet Propulsion Laboratory, Pasadena, CA, May 15, 1999.

7. J. R. Jensen, "A Plurality Voting Method for Acquisition of Regenerative Ranging Measurements," *2013 IEEE Aerospace Conference*, March 2-9, 2013, Big Sky, MT.
8. J. B. Berner and S. H. Bryant, "Operations Comparison of Deep Space Ranging Types: Sequential Tone vs. Pseudo-Noise," *2002 IEEE Aerospace Conference*, March 9-16, 2002, Big Sky, MT.
9. M. K. Reynolds, M. J. Reinhart, R. S. Bokulic, "A Two-Way Noncoherent Ranging Technique for Deep Space Missions," *2002 IEEE Aerospace Conference*, March 9-16, 2002, Big Sky, MT.
10. C. L. Thornton and J. S. Border, *Radiometric Tracking Techniques for Deep-Space Navigation*, Monograph 1 of the *Deep-Space Communications and Navigation Series*, Jet Propulsion Laboratory, Pasadena, CA, 2000.